Forensic Sci Med Pathol (2013) 9:163–169
DOI 10.1007/s12024-012-9398-y

ORIGINAL ARTICLE

Material differentiation in forensic radiology with single-source dual-energy computed tomography

Thomas D. Ruder · Yannick Thali · Stephan A. Bolliger · Sandra Somaini-Mathier · Michael J. Thali · Gary M. Hatch · Sebastian T. Schindera

Accepted: 3 December 2012 / Published online: 21 December 2012

Abstract The goal of this study was to investigate the use of dual-energy computed tomography (CT) in differentiating frequently encountered foreign material on CT images using a standard single-source CT scanner. We scanned 20 different, forensically relevant materials at two X-Ray energy levels (80 and 130 kVp) on CT. CT values were measured in each object at both energy levels. Intraclass correlation coefficient (ICC) was used to determine intra-reader reliability. Analysis of variance (ANOVA) was performed to assess significance levels between X-Ray attenuation at 80 and 130 kVp. *T* test was used to investigate significance levels between mean HU values of individual object pairings at single energy levels of 80 and 130 kVp, respectively. ANOVA revealed that the difference in attenuation between beam energies of 80 kVp compared to 130 kVp was statistically significant ($p < 0.005$) for all materials except brass and lead. ICC was excellent at 80 kVp (0.999, $p < 0.001$) and at 130 kVp (0.998, $p < 0.001$). *T* test showed that using single energy levels of 80 and 130 kVp respectively 181/190 objects pairs could be differentiated from one another based on HU measurements. Using the combined information from both energy levels, 189/190 object pairs could be differentiated. Scanning with different energy levels is a simple way to apply dual-energy technique on a regular single-energy CT and improves the ability to differentiate foreign bodies with CT, based on their attenuation values.

Keywords Forensic radiology · Identification · Foreign objects · Dual-energy CT · Single-source dual-energy CT · Virtopsy

T. D. Ruder (✉) · Y. Thali · M. J. Thali
Department of Forensic Medicine and Imaging, Institute of Forensic Medicine, University of Zurich, Winterthurerstrasse 190/52, 8057 Zurich, Switzerland
e-mail: thomas.ruder@irm.uzh.ch; thomas_ruder@hotmail.com

T. D. Ruder · S. T. Schindera
Institute of Diagnostic and Interventional Radiology, University Hospital Bern, Freiburgstrasse, 3010 Bern, Switzerland

T. D. Ruder · Y. Thali · S. Somaini-Mathier · G. M. Hatch
Center of Forensic Imaging and Virtopsy, Institute of Forensic Medicine, University of Bern, Buehlstrasse 20, 3012 Bern, Switzerland

S. A. Bolliger
Forensic Services, Department of Forensic Medicine, Cantonal Hospital, Aarau, Switzerland

S. A. Bolliger
Department of Forensic Pathology, Institute of Forensic Medicine, University of Bern, Buehlstrasse 20, 3012 Bern, Switzerland

S. Somaini-Mathier
Department of Diagnostic and Interventional Neuroradiology, University Hospital Bern, Freiburgstrasse, 3010 Bern, Switzerland

G. M. Hatch
Radiology-Pathology Center for Forensic Imaging, Departments of Radiology and Pathology, University of New Mexico, MSC07 4040, 1101 Camino de Salud NE, Albuquerque, NM 87102, USA

S. T. Schindera
Clinic for Radiology and Nuclear Medicine, University Hospital Basel, Petersgraben 4, 4031 Basel, Switzerland

Introduction

Less than a year after their discovery, X-Rays were used in the course of a forensic investigation to locate bullets in the neck of a fatally injured gunshot victim [1]. Since then, the detection, localization and identification of foreign bodies was the goal of many forensic radiologic examinations [2]. The introduction of cross-sectional imaging modalities to forensic medicine, most notably computed tomography (CT) [3–5], allowed for a more accurate localization of foreign materials than conventional radiographs [6]. The ability of CT to quantify X-Ray attenuation in Hounsfield Units (HU) [7, 8] is beneficial for the identification of objects. However, previous attempts to differentiate selected forensically relevant materials through HU measurements were limited by overlapping CT numbers [9, 10]. This limitation may be overcome by dual-energy CT (DECT).

In clinical imaging, DECT has a wide range of applications. It can be used to generate virtual non-contrast images, characterize atherosclerotic plaques, measure vascular perfusion of the brain, the heart, or the lungs, assess steatosis or iron overload in the liver, determine renal stone composition, detect bone bruise lesions, or reduce metal artifacts through monoenergetic image reconstruction [11–16]. Several of these clinical applications may also be implemented in forensic radiology. Dual-energy CT may be particularly useful to assess the composition of foreign objects within a corpse.

The behavior of individual materials at different X-Ray energy levels depends on their atomic number, the electron density, their density and their diameter [7, 8]. Knowing how a material behaves at different energy levels provides information about the composition of the material [12, 13, 15]. Currently, the most widely used dual-energy CT scanners are equipped with two X-Ray tubes that scan patients at two defined, different energy levels simultaneously [11, 15]. However, in the post-mortem setting, restrictions regarding radiation dose do not apply and dual-energy scans can be obtained with a single-source CT by scanning a corpse twice, at different energies levels [17] (Fig. 1).

The goal of this study was to assess the advantages of dual-energy CT regarding the differentiation of frequently encountered foreign materials using a standard single-source CT scanner.

Materials and methods

Materials

All 20 materials examined in this study were selected with regard to their potential forensic relevance, such as debris from motor vehicle accidents, shrapnel and fragments from explosions, projectiles from firearms, or jewelry for identification. The following materials were included: front and side windshield glass from a car, a block of tarmac, various rocks and other building materials (brick stone, tile, granite, quartzite, sandstone, slate, and cement), fragments of a windowpane, and a range of metals (aluminum, steel, brass, lead, silver and gold). All objects were placed in an anthropomorphic gelatin phantom with a gap of at least 2 cm between each object to avoid overlapping streak artifacts during CT.

Imaging protocol

Imaging was performed using a single-source, six-slice multi-detector row CT scanner (Somatom Emotion 6, Siemens, Forchheim, Germany). The phantom, containing all objects, was scanned at two different energy levels, first at 80 kVp (kilovolt peak), then at 130 kVp, always using a tube current time product of 130 mAs (milliampere second) collimation of 6 × 1 mm. Both scans were repeated three times on non-consecutive days of the same week. CT image reconstruction was performed with a slice thickness of 1.25 mm in increments of 0.7 mm, using bone-weighted tissue kernels and extended CT-scale. Extended CT-scale allows for HU measurements over an extended range, from −1,000 to +30,710 HU [18].

CT number measurements

All measurements were performed on a picture archiving and communication system (PACS) workstation (IDS7, Sectra, Linköping, Sweden). CT numbers were measured using a circular region of interest (ROI) tool (see Fig. 2). ROIs were placed manually by one reader (a doctoral student under the supervision of a radiologist with 5 years of experience). To ensure reliable HU measurements, each ROI included more than one pixel and ROIs were placed off the border of an object [19]. ROI measurements represent a very robust method and the accuracy and reliability of the ROI values is independent of a reader's experience [19]. All measurements were performed on all three individual scan series to account for possible tube voltage fluctuation between the different scan series. In addition, all measurements were repeated on the same position on three different slices (i.e., at different levels within an object) to account for possible heterogeneity of the material.

Statistics

Mean CT numbers were calculated for each material at 80 and 130 kVp. Intra-reader reliability was assessed with

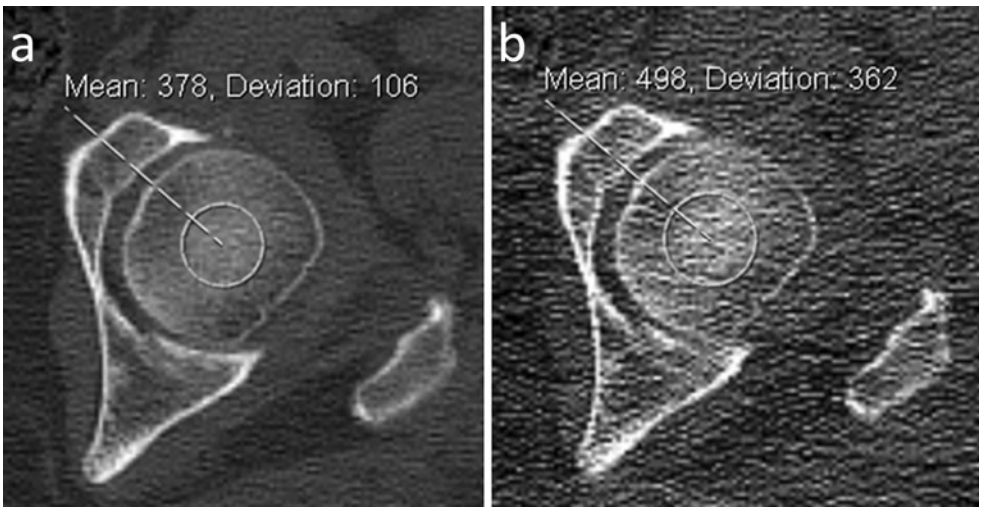

Fig. 1 Detail of a post-mortem CT (*left femur*) with CT number measurements in Houndsfield-Units (HU). The corpse was scanned twice: **a** was scanned at 130 kVp (*higher energy*), **b** was scanned at 80 kVp (*lower energy*). The bone attenuates the higher energy X-Ray beam (**a**) less than the lower energy X-Ray beam (**b**). HU depend on the energy of an X-Ray beam. Therefore the HU at 130 kVp is different (i.e., lower) than the HU at 80 kVp. Knowing how a material behaves at different energy levels provides information about the composition of the material

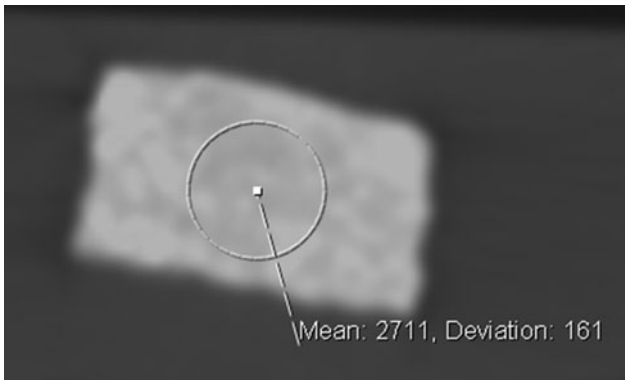

Fig. 2 CT image of sample material (block of granite). To ensure reliable HU measurements each region of interest (ROI) must be placed off the border an object (to avoid partial volume effect) and cover more than one pixel

intraclass correlation coefficient (ICC). An ICC of 1.0 indicates absolute agreement. Analysis of variance (ANOVA) was performed to assess significance levels (p) between X-Ray attenuation at 80 and 130 kVp. Additionally the t test was used to investigate the significance levels (p) between mean HU values of individual object pairings at 80 and 130 kVp, respectively. A p value <0.05 indicates statistical significance. The practical utility of dual-energy measurements was assessed through plotting individual CT numbers of every material in a dual-energy coordinate grid. The y-axis represents the HU at 80 kVp and the x-axis represents the HU at 130 kVp. For clarity, we used to separate grids for materials with CT numbers below and above 3,500 HU.

Table 1 Mean CT-Numbers in HU of all 20 materials at 80 and 130 kVp

Material	80 kVp	SD	130 kVp	SD
Car windshield (front)	2,011	300	1,650	208
Quartzite	2,137	81	1,708	61
Tile	2,205	119	1,685	56
Brick stone	2,262	77	1,615	58
Cement	2,287	165	1,667	117
Pottery	2,299	83	1,720	76
Sandstone	2,311	81	1,810	57
Windowpane	2,374	69	1,880	43
Car windshield (side)	2,518	104	1,987	48
Tarmac	2,722	394	2,029	274
Limestone	2,789	146	2,325	61
Granite	2,804	294	2,173	182
Aluminum	2,956	42	2,273	31
Marble	3,307	92	2,522	55
Slate	3,367	203	2,569	136
Silver	11,373	776	11,953	905
Gold	20,280	3943	22,624	3,554
Steel	29,366	722	19,635	331
Brass	30,710	0	28,138	920
Lead	30,710	0	30,710	0

SD standard deviation

Results

The mean CT numbers of the examined materials are listed in Table 1. All 20 materials can roughly be divided into two groups: one group (HU below 3,500) contains all

non-metallic objects and aluminum, the second group (HU above 10,000) contains exclusively metallic objects. Intra-reader reliability was excellent for both, ROI measurements at 80 and 130 kVp (ICC = 0.999, $p < 0.001$; and ICC = 0.998, $p < 0.001$, respectively). ANOVA revealed that the difference in attenuation between beam energies of 80 kVp compared to 130 kVp was statistically highly significant ($p < 0.005$) for all materials except brass ($p = 0.019$) and lead, where there was no difference in the attenuation at 80 and 130 kVp, respectively.

The *t* test revealed that there is a statistically significant difference between the individual CT numbers in a majority of the examined materials at both 80 and 130 kVp. Of the 190 possible combinations, only nine pairs of materials could not be differentiated relying on their CT numbers at 80 kVp. The HU of brick stone, cement, pottery, and sandstone were so close that none of these four materials could be distinguished from one another. In addition, sandstone could not be differentiated from windowpane and tile, and lead could not be distinguished from brass (Table 2). A similar result was found at 130 kVp: again nine pairs of materials could not be differentiated based on CT numbers at 130 kVp. Quartzite, tile, brick stone, and cement could all not be differentiated from the HU of the car windshield (front). Tile could not be distinguished from quartzite and cement. The three remaining undistinguishable pairs were: quartzite and pottery, sandstone and windowpane, and finally, car windshield (side) and tarmac (Table 3).

The dual-energy grid visualizes the differentiation of materials based on dual-energy CT (see Fig. 3). Materials that were not differentiable after a single energy scan may be distinguished with the additional information delivered by the second scan. For example brick stone, cement, pottery, and sandstone all feature HU around 2,300 at 80 kVp and are impossible to distinguish. However, at 130 kVp the individual attenuation of these four materials diverges enough to allow for a secure differentiation. Of all 190 possible combinations out of the 20 scanned materials, only one pair, i.e., sandstone and windowpane, could not be differentiated using the information of both scans.

Discussion

The results of our study show that dual-energy CT is a useful technique to distinguish different objects from one another on CT.

Objects with overlapping HU values at one energy level may be differentiated if their HU value is also measured at a second energy level. This observation stands in agreement with the findings from previous studies on dual-energy CT

Table 2 Differentiation of materials at 80 kVp

80 kVp	Marble	Pottery	Brass	Aluminium	Steel	Gold	Silver	Window pane	Car window front	Lead	Car window side	Granite	Cement	Quarzite	Tile	Tarmac	Brick	Limestone	Sandstone	Slate
Marble		S	S	S	S	S	S	S	S	S	S	S	S	S	S	S	S	S	S	S
Pottery			S	S	S	S	S	S	S	S	S	S	N	S	S	S	N	S	N	S
Brass				S	S	S	S	S	S	N	S	S	S	S	S	S	S	S	S	S
Aluminium					S	S	S	S	S	S	S	S	S	S	S	S	S	S	S	S
Steel						S	S	S	S	S	S	S	S	S	S	S	S	S	S	S
Gold							S	S	S	S	S	S	S	S	S	S	S	S	S	S
Silver								S	S	S	S	S	S	S	S	S	S	S	S	S
Window pane									S	S	S	S	S	S	S	S	S	S	N	S
Car window front										S	S	S	S	S	S	S	S	S	S	S
Lead											S	S	S	S	S	S	S	S	S	S
Car window side												S	S	S	S	S	S	S	S	S
Granite													S	S	S	S	S	S	S	S
Cement														S	S	S	N	S	N	S
Quarzite															S	S	S	S	S	S
Tile																S	S	S	N	S
Tarmac																	S	S	S	S
Brick																		S	N	S
Limestone																			S	S
Sandstone																				S
Slate																				

S = statistically significant difference between the mean CT numbers of two materials

N = statistically not significant difference between the mean CT numbers of two materials

Table 3 Differentiation of materials at 130 kVp

130 kVp	Marble	Pottery	Brass	Aluminium	Steel	Gold	Silver	Window pane	Car window front	Lead	Car window side	Granite	Cement	Quarzite	Tile	Tarmac	Brick	Limestone	Sandstone	Slate
Marble		S	S	S	S	S	S	S	S	S	S	S	S	S	S	S	S	S	S	S
Pottery			S	S	S	S	S	S	S	S	S	S	S	N	S	S	S	S	S	S
Brass				S	S	S	S	S	S	S	S	S	S	S	S	S	S	S	S	S
Aluminium					S	S	S	S	S	S	S	S	S	S	S	S	S	S	S	S
Steel						S	S	S	S	S	S	S	S	S	S	S	S	S	S	S
Gold							S	S	S	S	S	S	S	S	S	S	S	S	S	S
Silver								S	S	S	S	S	S	S	S	S	S	S	S	S
Window pane									S	S	S	S	S	S	S	S	S	S	N	S
Car window front										S	S	S	N	N	N	S	N	S	S	S
Lead											S	S	S	S	S	S	S	S	S	S
Car window side												S	S	S	S	N	S	S	S	S
Granite													S	S	S	S	S	S	S	S
Cement														S	N	S	S	S	S	S
Quarzite															N	S	S	S	S	S
Tile																S	S	S	S	S
Tarmac																	S	S	S	S
Brick																		S	S	S
Limestone																			S	S
Sandstone																				S
Slate																				

S = statistically significant difference between the mean CT numbers of two materials

N = statistically not significant difference between the mean CT numbers of two materials

[11, 12, 14, 15]. The usual restrictions regarding radiation dose do not apply in the post-mortem setting, and the repetition of a CT-scan with different scan parameters is a simple way to apply dual-energy technique using a standard single-source CT scanner [17].

We found that the combined information from the scan at 80 and 130 kVp allowed differentiating all 190 possible combinations of the 20 materials examined in this study except one single pair (sandstone and windowpane). This is not surprising, since the chemical basis of both these materials is quartz. After one scan only, it was not possible to distinguish the materials of nine pairs at 80 kVp and nine pairs at 130 kVp. For example, a complex material such as a car windshield was not distinguishable from quartzite, brick stone, tiles and cement at 130 kVp, but the addition of a scan at 80 kVp allowed for a reliable differentiation. The behavior of the individual materials at different energy levels depends on their atomic number, the electron density, their density and their diameter [7, 8]. Coursey et al. provide a comprehensible overview of the physical principles behind dual-energy CT and the interaction between radiation and matter [13].

There are a growing number of publications on application of DECT in clinical imaging [11–16]. So far, the potential of DECT has not yet been fully appreciated in forensic and post-mortem imaging. Our findings concur with Persson's statement that dual-energy CT may be used to characterize foreign bodies [17]. The application of the dual-energy technology could improve the results of earlier attempts with single-energy CT to identify materials through HU measurements. Bolliger et al. attempted to differentiate several forensically relevant objects and showed that metallic objects could be differentiated from non-metallic objects, but they encountered significant overlap between the mean HU values of several objects [9]. Jackowski worked extensively on dental identification and the possibilities to differentiate dental implants [18, 20]. Challenges they reported related to the differentiation of individual implants, might also be overcome through dual-energy CT.

ROI measurements have very high intra-reader reliability. Our measurements stand in agreement with the findings from previous studies [19].

Limitations

The selection of material may be criticized. The authors acknowledge that all materials examined in this study were selected arbitrarily. However, dual-energy technology relies on principles of radiation

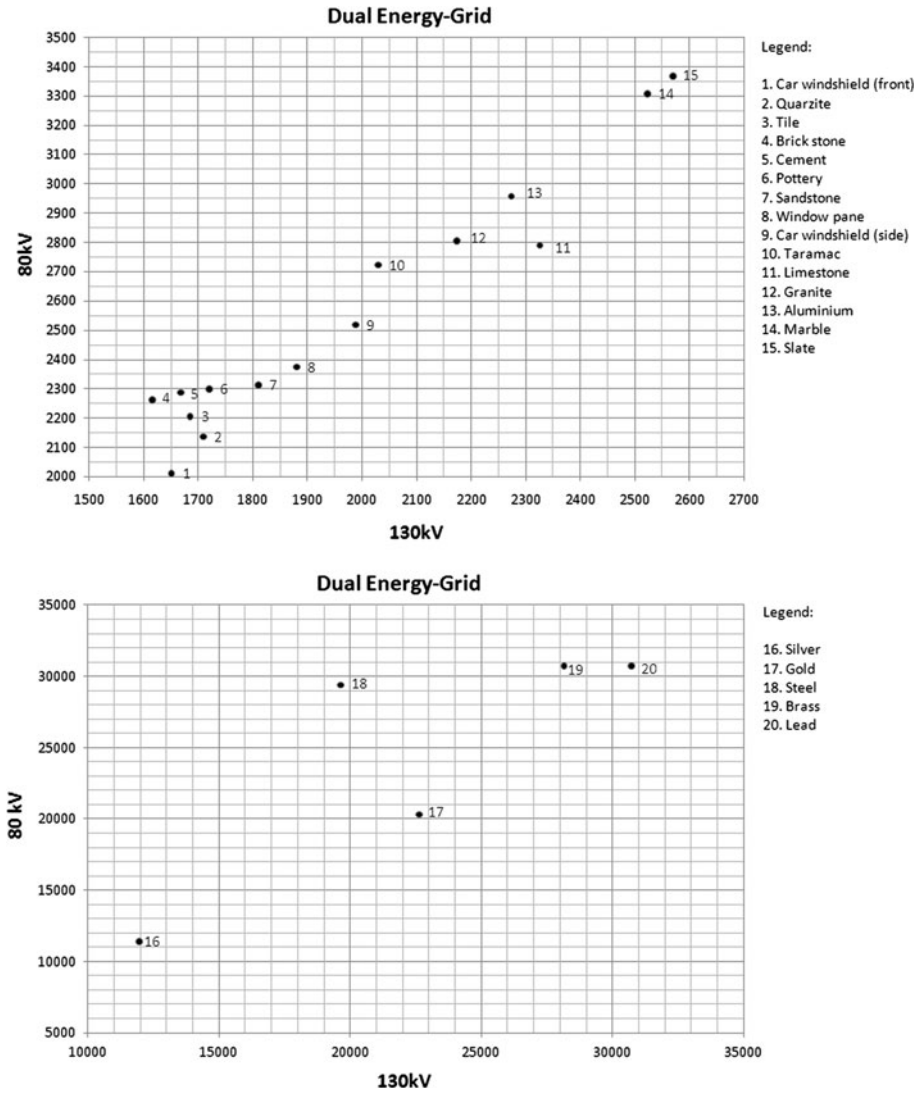

Fig. 3 The dual-energy grid allows for differentiation of materials that can not be distinguished at 80 or 130 kVp alone. The individual CT numbers of each material were plotted into the coordinate grid. The *y*-axis represents CT numbers at 80 kVp and the *x*-axis represents CT numbers at 130 kVp. For clarity, we used to separate grids for materials with CT numbers below and above 3,500 HU. *Example*: The CT numbers of material 6 (pottery, 2,299 HU) and material 7 (sandstone 2,311 HU) at 80 kVp are too close allow differentiation. However, at 130 kVp, the CT numbers of pottery (1,720 HU) and sandstone (1,810 HU) differ enough to distinguish the materials based on HU with dual-energy CT

physics and is, in theory, not dependent on the selection of absorbers. Nevertheless, HU measurements of metals can be quite challenging: metals are powerful absorbers of X-Rays. Thin copper plates, for example, are used as X-Ray filters in radiology and lead is used for protective aprons and shields in hospitals [7]. Because of their high density, metals are very powerful X-Ray absorbers and regularly induce artifacts on CT images that can negatively affect the reliability of HU measurements on both single- and dual-energy CT [21]. Therefore, one must be very careful when attempting to assess metallic objects with CT, even with dual-energy technique.

Conclusions

When a foreign object is detected in a corpse, single-energy CT can locate the object and allow for the assessment of its shape. With the addition of a second scan at a different energy level, conclusions regarding the composition of the object may be drawn. This additional piece of information may be especially useful when dealing with multiple cadavers in the setting of a mass disaster. The most relevant objects can be identified and forensic pathologists can be assisted in prioritizing the autopsy of those cases most likely to yield important forensic evidence.

Key points

1. Detection, localization, and identification of foreign objects are elementary scopes of forensic radiology.
2. Dual-energy CT has the ability to measure the X-Ray attenuation (in Hounsfield Units (HU)) of any absorber at two different energy levels and thus conclusions regarding the composition of an object may be drawn.

3. Dual-energy measurements can be performed on a standard single-source CT scanner if an object or cadaver is scanned twice at different energy levels.
4. Single-source dual-energy CT scanning increases the ability of object differentiation and identification through provides additional information regarding combined information from two energy levels.

References

1. Brogdon BG, Lichtenstein JE. Forensic radiology in historical perspective. In: Brogdon BG, editor. Forensic radiology. Boca Raton: CRC Press; 1998. p. 13–34.
2. Brogdon BG, Lichtenstein JE. Scope of forensic radiology. In: Brogdon BG, editor. Forensic radiology. Boca Raton: CRC Press; 1998. p. 35–52.
3. Thali MJ, Yen K, Schweitzer W, Vock P, Boesch C, Ozdoba C, Schroth G, Ith M, Sonnenschein M, Doernhoefer T, Scheurer E, Plattner T, Dirnhofer R. Virtopsy, a new imaging horizon in forensic pathology: virtual autopsy by postmortem multislice computed tomography (MSCT) and magnetic resonance imaging (MRI)—a feasibility study. J Forensic Sci. 2003;48:386–403.
4. Rutty GN, Morgan B, O'Donnell C, Leth PM, Thali M. Forensic institutes across the world place CT or MRI scanners or both into their mortuaries. J Trauma. 2008;65:493–4.
5. Thali MJ, Dirnhofer R, Vock P. The virtopsy approach. 1st ed. Boca Raton: CRC Press Taylor & Francis Group; 2009.
6. O'Donnell C, Iino M, Mansharan K, Leditscke J, Woodford N. Contribution of postmortem multidetector CT scanning to identification of the deceased in a mass disaster: experience gained from the 2009 Victorian bushfires. Forensic Sci Int. 2011;205:15–28.
7. Weissleder R, Wittenberg J, Harisinghani MG, Chen JW. Imaging Physics. In: Weissleder R, Wittenberg J, Harisinghani MG, Chen JW, editors. Primer of diagnostic imaging. Philadelphia: Mosby Elsevier; 2007. p. 989–1069.
8. Huda W, Slone R. Computed tomography. In: Huda W, Slone R, editors. Review of radiologic physics. Philadelphia: Lippincott Williams & Wilkins; 2003. p. 121–36.
9. Bolliger SA, Oesterhelweg L, Spendlove D, Ross S, Thali MJ. Is differentiation of frequently encountered foreign bodies in corpses possible by Hounsfield density measurement? J Forensic Sci. 2009;54:1119–22.
10. Jackowski C, Lussi A, Classens M, Kilchoer T, Bolliger S, Aghayev E, et al. Extended CT scale overcomes restoration caused streak artifacts for dental identification in CT-3D color encoded automatic discrimination of dental restorations. J Comput Assist Tomogr. 2006;30:510–3.
11. Flohr TG, McCollough CH, Bruder H, Petersilka M, Gruber K, Süss C, et al. First performance evaluation of a dual-source CT (DSCT) system. Eur Radiol. 2006;16:256–68.
12. Johnson TR, Krauss B, Sedlmair M, Grasruck M, Bruder H, Morhard D, et al. Material differentiation by dual energy CT: initial experience. Eur Radiol. 2007;17:1510–7.
13. Coursey CA, Nelson RC, Boll DT, Paulson EK, Ho LM, Neville AM, et al. Dual-energy multidetector CT: how does it work, what can it tell us, and when can we use it in abdominopelvic imaging? Radiographics. 2010;30:1037–55.
14. Pache G, Krauss B, Strohm P, Saueressig U, Blanke P, Bulla S, Schäfer O, Helwig P, Kotter E, Langer M, Baumann T. Dual-energy CT virtual noncalcium technique: detecting posttraumatic bone marrow lesions–feasibility study. Radiology. 2010;256:617–24.
15. Johnson TRC, Fink C, Schönberg SO, Reiser MF. Dual energy CT in clinical practice. 1st ed. Berlin: Springer; 2011.
16. Guggenberger R, Winklhofer S, Osterhoff G, Wanner GA, Fortunati M, Andreisek G, Alkadhi H, Stolzmann P. Metallic artefact reduction with monoenergetic dual-energy CT: systematic ex vivo evaluation of posterior spinal fusion implants from various vendors and different spine levels. Eur Radiol. 2012;22:2357–64.
17. Persson A, Jackowski C, Engström E, Zachrisson H. Advances of dual source, dual-energy imaging in postmortem CT. Eur J Radiol. 2008;68:446–55.
18. Jackowski C, Thali MJ. Radiologic Identification. In: Thali MJ, Dirnhofer R, Vock P, editors. The virtopsy approach. Boca Raton: CRC Press Taylor & Francis Group; 2009. p. 169–85.
19. Ruder TD, Thali Y, Schindera ST, Dalla Torre SA, Zech WD, Thali MJ, Ross S, Hatch GM. How reliable are Hounsfield-unit measurements in forensic radiology? Forensic Sci Int. 2012;220:219–23.
20. Woisetschläger M, Lussi A, Persson A, Jackowski C. Fire victim identification by post-mortem dental CT: radiologic evaluation of restorative materials after exposure to high temperatures. Eur J Radiol. 2011;80:432–40.
21. Barrett JF, Keat N. Artifacts in CT: recognition and avoidance. Radiographics. 2004;24:1679–91.